

A note on the production of photons at RHIC ¹

Stefano Frixione^a

^aCERN, TH division, Geneva, Switzerland

I study the production of prompt photons in polarized hadronic collisions, considering different isolation prescriptions. In particular, I focus on the problem of the measurability of the polarized gluon density in the proton through isolated-photon data.

1. Isolated-photon cross sections

The study of the production of prompt photons in hadronic collisions is a very promising tool in at least two respects: first, it can be helpful in the investigation of the underlying parton dynamics and second, it is the (almost) only way to directly measure the gluon density of the nucleons at intermediate and large x 's. Although the cross section for prompt-photon production is sizeably smaller than that for jet or single-inclusive hadron production, the signal of the former process is much cleaner than that of the latter processes. This is basically due to the fact that the photon can couple directly only to quarks, and not to gluons. This implies that, at the leading order in perturbative QCD, only two partonic processes, namely $qg \rightarrow \gamma q$ and $q\bar{q} \rightarrow \gamma g$, contribute to prompt-photon cross section, as opposed to the larger number of processes in the case of jet production.

Unfortunately, the cleanliness of the prompt-photon signal is limited by the fact that, as is well known, photons can also be produced through a fragmentation process. In such a process, a quark or a gluon, produced in a pure-QCD reaction, fragments into a photon plus a number of hadrons. Furthermore, prompt photons have a dominant background due to the production of neutral pions, with the subsequent decay $\pi^0 \rightarrow \gamma\gamma$. The problem of background rejection is very effectively solved by requiring the photon to be isolated from energetic hadron tracks in a 'small' region surrounding the photon itself. The nature of this region depends upon the type of

the particles that initiate the scattering process: in e^+e^- collisions, it is a cone of fixed aperture drawn around the photon axis, while in hadronic collisions it is a subset of the pseudorapidity-azimuthal angle plane, whose centre is given by the pseudorapidity and azimuthal angle of the photon. The difference in the definitions is due to the fact that, in the case of hadronic collisions, one necessarily needs a prescription invariant under longitudinal boosts. Apart from greatly reducing the background-to-noise ratio, the isolation condition also diminishes the contribution to the cross section coming from the fragmentation mechanism, relative to the contribution of the direct mechanism, in which the photon participates in the hard scattering. This is due to the fact that, in the fragmentation process, the photon and the companion hadrons, generated by the fragmentation of the same parton, are usually close to each other (fragmentation is essentially collinear), while in the direct process the photon is usually well separated from other hadrons (at the leading order, the photon and the recoiling hadron are back-to-back in the transverse-momentum plane, because of the necessity of momentum conservation).

In order to sensibly compare the data with the theoretical predictions, it is essential that the very same isolation prescription is applied both in the experimental analysis and in the computation of the cross sections. From the theoretical point of view, this poses additional problems with respect to the case of fully-inclusive photon production, since the calculations are technically more involved, especially for the fragmentation component. In general, when going beyond

¹Talk given at QCD99, 7-13 July 1999, Montpellier, F.

leading order in QCD, the direct and the fragmentation contributions are not separately well defined, both being divergent order by order in perturbation theory. In the direct part, the divergence arises from the collinear splitting of a quark into a photon and a quark. Such a singularity is only cancelled by means of the bare parton-to-photon fragmentation functions, which enter the fragmentation contribution. Thus, even for very tight isolation prescriptions, the isolated-photon cross section depends upon the fragmentation mechanism. However, an isolation definition has been proposed [1], which is such that the cross section gets contribution only from the direct mechanism, and still is well defined at all orders in perturbation theory. This is seemingly incompatible with what stated above concerning the cancellation of the QED collinear singularity. However, with the definition of ref. [1], the direct contribution is free of quark-photon collinear singularities. Loosely speaking, this is achieved by requiring the energy of a parton to be smaller and smaller the closer the parton is to the photon, until eventually only zero-energy partons are allowed exactly collinear to the photon. In this way, the vanishing energy of the quark damps the quark-photon collinear singularity. More precisely, the isolation prescription of ref. [1] is given as follows: drawing a cone of half-angle R_0 around the photon axis in the $\eta-\phi$ plane (isolation cone), and denoting by $E_{T,had}(R)$ the total amount of transverse hadronic energy inside a cone of half-angle R , the photon is isolated if the following inequality is satisfied:

$$E_{T,had}(R) \leq \epsilon_\gamma p_{T\gamma} \mathcal{Y}(R), \quad (1)$$

for all $R \leq R_0$. Here, $p_{T\gamma}$ is the transverse momentum of the photon. The function \mathcal{Y} can be rather freely chosen, provided that it vanishes fast enough for $R \rightarrow 0$. A sensible choice is the following:

$$\mathcal{Y}(R) = \left(\frac{1 - \cos R}{1 - \cos R_0} \right)^n, \quad n = 1. \quad (2)$$

Notice that this isolation prescription is rather similar to the ordinary cone prescription [2], which is obtained by imposing:

$$E_{T,had}(R_0) \leq \epsilon_c p_{T\gamma}. \quad (3)$$

Indeed, eq. (3) can be recovered from eqs. (1) and (2) by setting $n = 0$ and $\epsilon_\gamma = \epsilon_c (E_{T,had}(R))$ is by construction a function monotonically increasing with R). The isolation prescriptions given in eqs. (1) and (3) have been proven to be infrared safe. More details can be found in refs. [1,3]

2. Photon production in polarized pp collisions

The isolation prescriptions given above apply to any kind of hadron-hadron scattering. With only minor modifications (the isolation cone is drawn in the physical 3-space, and the transverse energy is substituted with the energy), they can also be used in e^+e^- collisions. In the following, I will present phenomenological predictions relevant to polarized pp collisions, in the energy range of the BNL collider RHIC ($\sqrt{S} = 200-500$ GeV). All the results given in this paper are accurate to next-to-leading order in QCD. A much more detailed and thorough discussion can be found in ref. [4].

One of the main goals of the collider RHIC will be that of extracting the polarized gluon density in the proton, Δg , from prompt-photon data. This will be done by comparing the experimental results with the cross sections computed at the highest possible order in perturbation theory (which is at present the next-to-leading one). It is therefore crucial to understand if the theoretical predictions for isolated-photon production are reliable. This is not trivial, since the isolation cuts are effective only on the radiative-emission contribution to the cross section, while the virtual corrections are not affected by them; this means that the cancellation of the infrared divergencies is perturbed by the isolation, regardless of the fact that the isolation prescription is formally infrared safe. As is customary in the cases in which a next-to-next-to-leading order computation is not available, the perturbative stability of the results can only be studied by looking at dependence of the physical observables upon the renormalization and factorization scales. As was shown in ref. [4], isolated-photon cross sections at RHIC appear to be under good perturbative control, both for inclusive isolated-photon

and for photon-plus-jet observables. This conclusion holds for both the isolation prescriptions of eqs. (1) and (3). It turns out that, when varying the scales between half and twice their default values, the cross sections change at the most by a factor of 15% (10%) at the leading (next-to-leading) order. It is therefore clear that the inclusion of the radiative corrections improves the stability of the results, thus implying a non-pathological behaviour of the perturbative expansion.

Having established that the predictions of perturbative QCD can be sensibly used in a comparison with data, I now turn to the issue of the dependence of the isolated-photon cross sections upon the polarized parton densities, in order to answer the question of whether the measurements performed at RHIC will be useful in order to pin down the presently poorly known Δg . The best tool to this end is the asymmetry cross section \mathcal{A} ; in fact, many systematic uncertainties cancel out in the ratio of polarized and unpolarized cross sections. The measurability of a spin asymmetry for a given process, as far as statistics is concerned, is of course determined by the counting rate. The quantity

$$(\mathcal{A})_{min} = \frac{1}{P^2} \frac{1}{\sqrt{2\sigma\mathcal{L}\epsilon}} \quad (4)$$

can be regarded as the minimal asymmetry that can be detected experimentally or, equivalently, as the expected statistical error of the measurement, for a given integrated luminosity relevant to parallel or antiparallel spins of the incoming particles, \mathcal{L} , beam polarizations P and a detection efficiency $\epsilon \leq 1$; σ is the unpolarized cross section integrated over a certain range in the observable under study. Eq. (4) can be obtained starting from the requirement that the asymmetry be larger than its statistical error. The simplest way to do so is to compute the statistical error affecting the quantity $(N^{\vec{\zeta}} - N^{\bar{\zeta}})/(N^{\vec{\zeta}} + N^{\bar{\zeta}})$, where N is the number of production events for a given spin configuration (of the incoming particles). This quantity coincides with the asymmetry in the hypothesis in which the integrated luminosities for different spin configurations are equal, which I assume here. With a straightforward computation, assuming the sta-

tistical error on N to be \sqrt{N} , and neglecting a factor of the order of $\sqrt{1 - \mathcal{A}^2}$, one gets immediately eq. (4).

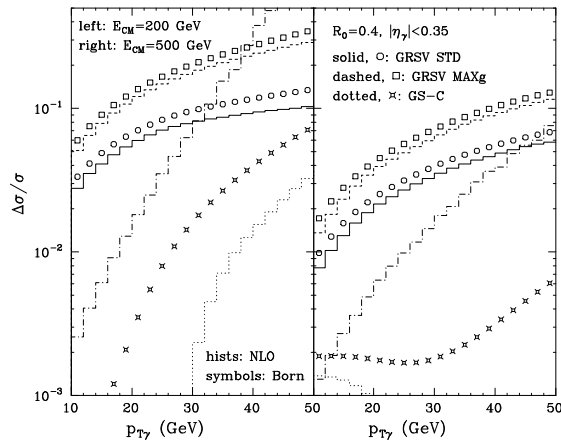


Figure 1. Asymmetry as a function of $p_{T\gamma}$, for $\sqrt{S} = 200$ GeV (left) and 500 GeV (right).

In fig. 1 I present the asymmetry as a function of the photon transverse momentum, for different centre-of-mass energies of the colliding protons. A cut $|\eta_\gamma| < 0.35$ on the photon pseudorapidity has been applied, and the isolation prescription of eq. (1) has been adopted. Both the next-to-leading order (histograms) and the leading order (symbols) results are shown. The asymmetries have been computed with three different parametrizations for the parton densities. The GRSV STD set [5] (which results in the solid histograms) is the ‘best fit’ (within the assumptions of the authors) to the presently available data on polarized structure functions. The GRSV MAXg [5] and GS-C [6] sets (which result in the dashed and in the dotted histograms respectively) have on the other hand to be considered as the two most extreme choices compatible with the structure function data, thus giving an estimate of the largest possible spread for the predictions of the asymmetry. Finally, the dot-dashed his-

tograms depict the minimally observable asymmetry as given in eq. (4), for $\mathcal{L} = 100 \text{ pb}^{-1}$, $P = 1$ and $\epsilon = 1$, and with the unpolarized cross section integrated over a $p_{T\gamma}$ bin of width equal to 2 GeV. From the figure, we see that the shapes of the asymmetries obtained using the GRSV STD and GRSV MAXg sets are quite similar, but the difference in normalization is sizeable. On the other hand, the result obtained with GS-C looks completely different; the asymmetry turns negative over a certain $p_{T\gamma}$ range at the next-to-leading order. It is clear that, if the parton densities are similar to those of the GS-C set, it will be rather difficult to get a non-zero signal for the asymmetry at RHIC. A more favourable situation can be found if a larger pseudorapidity range is considered ($-1 < \eta_\gamma < 2$). The minimally observable asymmetry decreases by a factor that can be as large as 2, and the asymmetry obtained with GS-C sizeably increases, becoming larger than $(\mathcal{A})_{min}$ in the low- $p_{T\gamma}$ region.

It is instructive to compare the asymmetries at the two different centre-of-mass energies considered in fig. 1. We can observe that, as is well known, at smaller centre-of-mass energies the asymmetries are generally larger. However, when comparing the predicted asymmetries with the minimally observable asymmetry, it is clear that, at a fixed value of $p_{T\gamma}$, and except for the first few $p_{T\gamma}$ bins, the situation at $\sqrt{S} = 500 \text{ GeV}$ is more favourable than that at $\sqrt{S} = 200 \text{ GeV}$. On the other hand, as far as the measurement of Δg at a given x is concerned, one should rather look at the asymmetries at fixed $x_T^\gamma = 2p_{T\gamma}/\sqrt{S}$, since this corresponds to the value at which the parton densities are probed predominantly. Then, the quantity deciding about which energy is more favourable, is the minimally observable asymmetry at a given x_T^γ . For $\sqrt{S} = 500 \text{ GeV}$, one finds a value of $(\mathcal{A}_{p_{T\gamma}})_{min}$ larger than for the lower energy, making the higher-energy option appear less favourable. However, two points should be kept in mind here: firstly, in both plots in fig. 1 the same value for the integrated luminosity has been used, whereas in reality one anticipates a higher (by a factor of 2 to 3) luminosity for $\sqrt{S} = 500 \text{ GeV}$. Secondly, the lower cut-off for $p_{T\gamma}$ will certainly

be the same for both energies, which means that at $\sqrt{S} = 500 \text{ GeV}$ one can explore a region of x_T^γ that is inaccessible at $\sqrt{S} = 200 \text{ GeV}$.

The same asymmetries as presented above have been computed adopting the isolation prescription of eq. (3). Only negligible differences were found in the case of the GRSV density sets, while some difference can be observed, in the case of the GS-C set, in the central η_γ region, where the asymmetry obtained with eq. (3) is smaller than that obtained with eq. (1). Also, asymmetries were computed, for both isolation prescriptions, as a function of quantities defined in terms of the photon and of the recoiling jet variables. In general, and as far as the statistics is concerned, inclusive-photon measurements seem to be somewhat more favourable than photon-plus-jet ones. More details can be found in ref. [4].

Acknowledgements

The results presented in this paper have been obtained in collaboration with W. Vogelsang, whom I warmly thank. The partial financial support by the University of Montpellier is gratefully acknowledged.

REFERENCES

1. S. Frixione, *Phys. Lett.* **B429**(1998)369.
2. H. Baer, J. Ohnemus and J. F. Owens, *Phys. Rev.* **D42**(1990)61; P. Aurenche, R. Baier and M. Fontannaz, *Phys. Rev.* **D42**(1990)1440; E.L. Berger and J. Qiu, *Phys. Rev.* **D44**(1991)2002; E. W. N. Glover and W. J. Stirling, *Phys. Lett.* **B295**(1992)128; Z. Kunszt and Z. Trocsanyi, *Nucl. Phys.* **B394**(1993)139; L.E. Gordon and W. Vogelsang, *Phys. Rev.* **D50**(1994)1901.
3. S. Catani, M. Fontannaz and E. Pilon, *Phys. Rev.* **D58**(1998)094025.
4. S. Frixione and W. Vogelsang, preprint CERN-TH/99-247, YITP-99-47, hep-ph/9908387, to appear in *Nucl. Phys.* **B**.
5. M. Glück, E. Reya, M. Stratmann and W. Vogelsang, *Phys. Rev.* **D53**(1996)4775.
6. T. Gehrmann and W.J. Stirling, *Phys. Rev.* **D53**(1996)6100.